

Kinetics of methyl methacrylate (MMA) combustion assessed by time-resolved speciation behind shock waves

Nicholas M. Kuenning*, Isabelle C. Sanders[†], Tara Mellor[‡], Nicolas Q. Minesi[§], R. Mitchell Spearrin[¶] *University of California, Los Angeles (UCLA), Los Angeles, CA 90095, USA*

Daniel I. Pineda The University of Texas at San Antonio (UTSA), San Antonio, TX 78249, USA

In this work, laser absorption spectroscopy is employed to study reaction kinetics of methyl methacrylate (MMA) decomposition and oxidation through species time-history measurements of formaldehyde (CH₂O), carbon monoxide (CO), and carbon dioxide (CO₂) behind reflected shock waves. The optical strategy probes a cluster of rovibrational transitions in the Q-branches of the ν_1 fundamental band and the $\nu_2+\nu_4$ combination band of CH₂O near 3.60 µm, a cluster of rovibrational transitions in the P-branch of the fundamental band of CO near 4.98 µm, and a transition in the R-branch of the $(01^00\to01^01)~\nu_3$ band of CO₂ near 4.19 µm. Initial spectroscopic measurements were conducted using a scanned-wavelength direct absorption technique behind reflected shock waves in a high-enthalpy shock tube to measure spectrally-resolved absorption cross-sections of CH₂O for conditions spanning 850–1550 K and 1.0–2.0 atm. These cross-section data, along with established two-line thermometry techniques, are subsequently used to infer CH₂O, CO, and CO₂ mole fraction during the pyrolysis and oxidation of shock-heated MMA/oxygen mixtures. These data provide valuable experimental constraints on MMA pyrolysis and oxidation chemical models employed in poly(methyl methacrylate) (PMMA) hybrid rocket combustion applications.

I. Nomenclature

P = pressure

T = temperature

X = mole fraction

 α = spectral absorbance

I = light intensity

L = optical pathlength

 S_j = line-strength of transition j σ = absorption cross-section

II. Introduction

Hybrid rocket engines, comprising fuel and oxidizer propellants stored in different phases of matter (e.g., solid, liquid, gas), have numerous safety, cost, and theoretical performance advantages over many bi-propellant liquid and solid chemical propulsion systems, and have recently received significant attention for potential use in interplanetary missions and in-space propulsion systems [1–5]. In practice, however, they have historically exhibited sub-optimal combustion performance, particularly when operating on low-regression-rate, polymer-based fuels [6, 7], rendering them impractical for most propulsion applications in industry. To accurately assess performance limitations and identify pathways to

^{*}Graduate Student Researcher, Mechanical and Aerospace Engineering Department

[†]Ph.D. Candidate, Mechanical and Aerospace Engineering Department, AIAA Member

[‡]Undergraduate Student Researcher, Mechanical and Aerospace Engineering Department

[§]Postdoctoral Scholar, Mechanical and Aerospace Engineering Department

[¶]Associate Professor, Mechanical and Aerospace Engineering Department, AIAA Member

Assistant Professor, Mechanical Engineering Department, AIAA Member

improvements for hybrid rocket engines, chemical kinetic investigations are needed to characterize combustion progress and reaction mechanisms of hybrid rocket propellants and their decomposition products.

Owing to its relatively simple depolymerization and thermal decomposition behavior, poly(methyl methacrylate) (PMMA) has been studied for several decades by both the fire science and propulsion communities [8–16]. Since the pyrolysis kinetics of PMMA are not complicated by charring or cross-linking behavior, its constituent monomer methyl methacrylate (MMA, C₅H₈O₂) accounts for nearly 95% of its pyrolysis products, historically providing a tractable and accessible modeling framework for PMMA combustion. The gas-phase reaction chemistry of MMA decomposition and oxidation is less well-characterized, however, and in-situ speciation data in the literature are scarce. Most experimental kinetic investigations of MMA have focused on determining laminar flame speeds and collecting spatially-resolved concentration profiles of multiple species in laminar flames [8, 17–20], wherein the destruction of the fuel molecules is achieved mainly through H-abstraction reactions readily enabled by an abundance of radicals provided by the flame zone. The chemical kinetics of ignition are radically distinct from flames [21], however, and are particularly relevant in turbulent flame regimes [22] which typically dominate rocket propulsion applications. To the authors' knowledge, no decomposition or ignition studies involving time-resolved speciation have been performed for MMA, leaving significant validation gaps for existing chemical models. Figure 1 shows predictions of species time histories for MMA decomposition at multiple temperatures using two different reaction mechanisms (a full mechanism [19] and a reduced mechanism [23] developed using the full mechanism as a reference) validated against experimental data from flames, demonstrating significant disagreements (orders of magnitude in time) for MMA, CH₂O, CO₂, and CO time-histories. These differences in predictions motivate the need for time-resolved measurements of species time-histories to further constrain models of MMA decomposition.

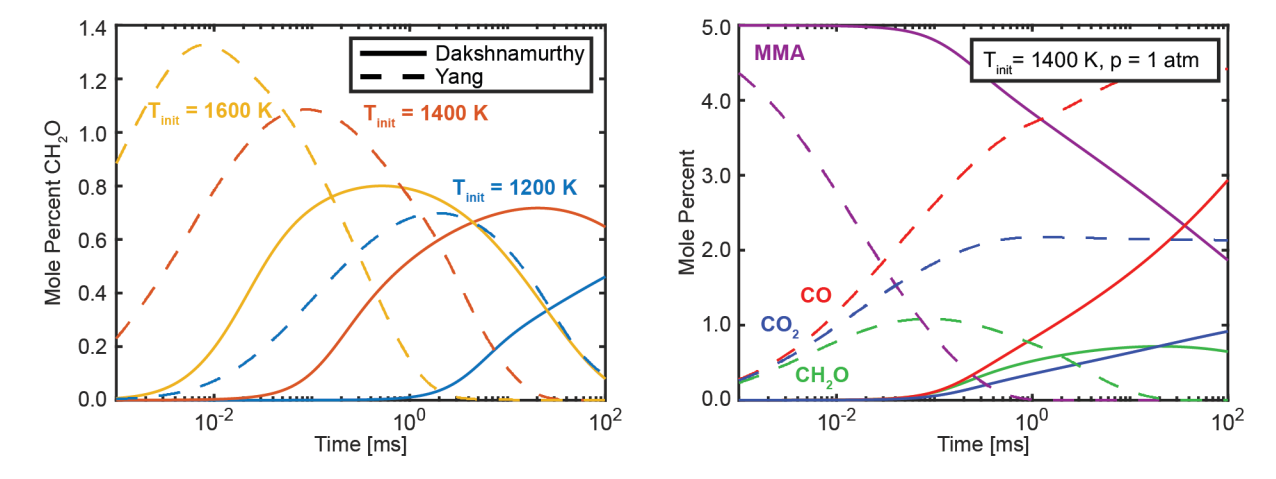


Fig. 1 Predicted time evolutions of CH_2O mole percent at a range of temperatures (left) and other relevant species at a fixed temperature (right) from a 5% initial concentration of MMA diluted in argon at a pressure of 1 atm using the chemical models by Yang et al. [19] and Dakshnamurthy et al. [23].

Accurate prediction of reactant, intermediate, and product species evolution in combustion systems is critical for the development of practical chemical propulsion devices, owing to their relevance to overall fuel-specific impulse (governed by exhaust molecular weight and flame temperature) and combustion chamber design (driven by required residence time) [24]. The predictive capability of fuel oxidation models can be evaluated in the laboratory through comparison with time-resolved species measurements behind incident and reflected shock waves, often through optically-based measurement methods such as laser absorption spectroscopy (LAS). Along with ignition delay times and flame speeds—which are aggregate measurements of overall combustion behavior—quantitative species time-histories recorded by LAS can provide an additional powerful constraint on kinetic models [25]. Formaldehyde (CH₂O) is an important early intermediate combustion species in the oxidation of nearly all hydrocarbon fuels, and carbon monoxide (CO) is the last carbon-containing species preceding complete combustion to carbon dioxide (CO₂). Measurements of these species' time-histories can provide valuable experimental constraints on chemical models aimed at describing many combustion processes, including hybrid rocket propulsion wherein PMMA is the solid fuel.

This work details the implementation of a laser absorption spectroscopic method to measure CH₂O, CO, CO₂ and temperature in shock-heated methyl methacrylate (MMA) decomposition and oxidation experiments. It is envisioned

that time-resolved measurements performed in shock tube studies can help anchor simulations and improve kinetic predictions of CH₂O, CO, and CO₂ evolution and, in turn, improve the accuracy and robustness of state-of-the-art chemical mechanisms for MMA decomposition and oxidation.

III. Experimental Methods

A. Laser Absorption Spectroscopy

Laser absorption spectroscopy (LAS) is a well-established optical diagnostic technique for shock tube kinetics studies, owing to its high time-resolution, species specificity, and quantitative capability in the measurement of species and temperature [25]. Spectral absorbance $\alpha(\nu)$ of species measured in this work is calculated using the ratio of transmitted light (I_t) to incident light (I_0) as defined by two different forms of the Beer-Lambert law:

$$\alpha(\nu) = -\ln\left(\frac{I_t}{I_0}\right)_{\nu} = PX_{abs}S_i(T)\varphi_i(\nu)L = \sigma_{abs}(\nu, P, T)LN_{abs}$$
 (1)

In the first form, P [atm] is the total pressure, X_{abs} is the absorbing species mole fraction, $S_i(T)$ [cm⁻²/atm] is the linestrength for rovibrational transition i at temperature T[K], and L[cm] is the absorption pathlength. In the second form, $\sigma_{abs}(v, P, T)$ [cm²/molecule] is the absorbing species cross-section (dependent on wavenumber ν [cm⁻¹], which is dependent on pressure P [atm] and temperature T [K]), and N_{abs} [molecules/cm³] is the absorbing species number density. The first form is typically employed when a comprehensive line-by-line spectral database of an absorbing species is confidently known and the spectral transitions i are easily separable in the absorbance measurement. This form is used in the present study to evaluate the concentration of CO and CO₂, and is discussed at length in prior work [14, 15]. The second cross-section formulation of the Beer-Lambert law is appropriate for broadly-absorbing species for which the temperature-dependent line-by-line spectroscopy is less well-known and/or the absorbance spectra are convoluted enough to preclude identification of individual spectral transitions from the absorbance measurement. An example of this is provided in Fig. 2, which shows predictions of the heavily convoluted absorbance spectra of CH₂O near 3.6 µm alongside the relatively isolated ro-vibrational transitions of CO₂ and CO near 4.2 µm and 5.0 µm, respectively. In this study, we employ this second form of the Beer-Lambert law to evaluate the concentration of CH₂O, first developing a database of spectrally-resolved cross-sections $\sigma_{abs}(v, P, T)$ at multiple pressures and temperatures as described in Section III.C. We then leverage this cross-section database to quantitatively interpret CH₂O absorbance spectra measured during the decomposition and oxidation of shock-heated methyl methacrylate. Spectroscopic measurements of CO and CO₂ are simultaneously performed with line-by-line interpretation.

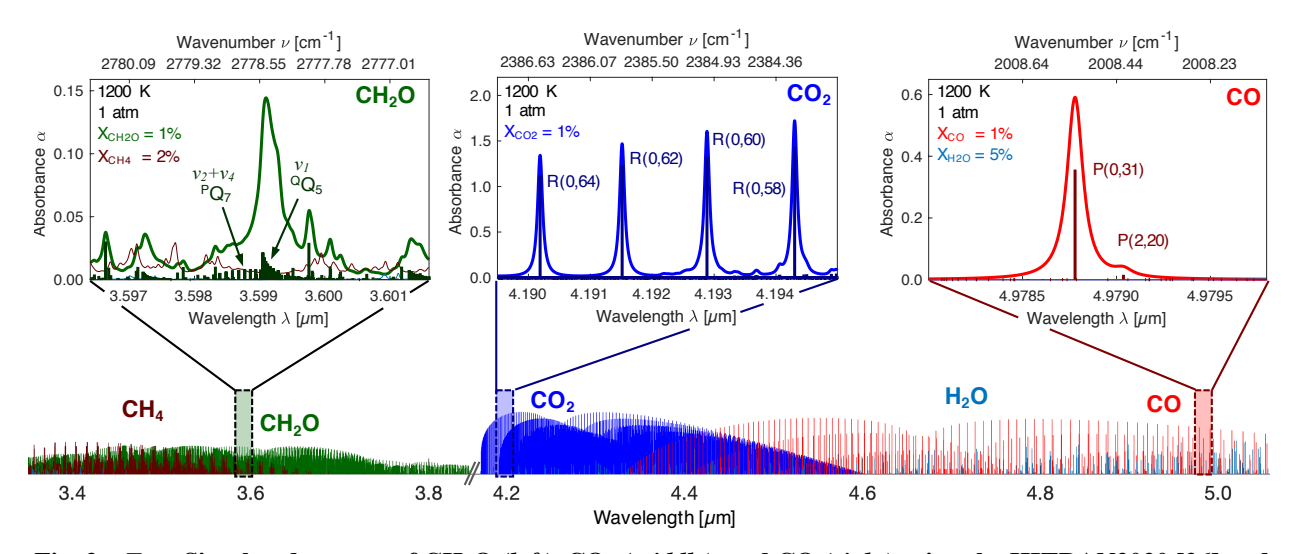


Fig. 2 *Top:* Simulated spectra of CH₂O (*left*), CO₂ (*middle*), and CO (*right*) using the HITRAN2020 [26] and HITEMP databases [27]; *Bottom:* Broadband spectral simulations of targeted species and potential interferers.

B. Experimental and Optical Setup

The high-temperature measurements for this study are performed behind reflected shock waves in the High Enthalpy Shock Tube (HEST) at UCLA, described in previous work [28, 29] and depicted in Fig. 3. The facility comprises a high-pressure driver section and a low-pressure driven (test gas) section, which are separated by a polycarbonate diaphragm. The test section of the shock tube has a pathlength of L = 10.32 cm and is circumscribed by interchangeable ports holding either sensors or optical windows 2 cm from the end wall. For all experiments, reflected shock pressure in the shock tube test section is measured directly with a dynamic pressure transducer (Kistler 601B1) via a charge amplifier (Kistler 5018A) and temperature is inferred from the shock wave speed determined via time of arrival sensors (Dynasen, Inc.) along the shock tube. Uncertainties in reflected shock test conditions are typically about 1% when properly accounting for vibrational relaxation of all components of the test gas [30].

The shock tube is connected to vacuum pumps, an agitated mixing tank, and a gas delivery manifold used to barometrically prepare the mixtures of interest for all experiments using dual-capacitance heated manometers (MKS Baratron 627B). Notably, the gas delivery manifold is also connected to an interchangeable glass flask containing either solid or liquid chemicals from which gaseous vapors are evaporated and mixed with either inert or oxidizing gases during preparation of the test gas mixtures of interest. For characterizing the high-temperature spectroscopy behavior of CH_2O near 3.6 μ m, mixtures of 1,3,5 Trioxane ($C_3H_6O_3$) and argon (Ar) were prepared for shock-heating across a range of temperatures and pressures. $C_3H_6O_3$, when shock-heated, decomposes into three CH_2O molecules [31], providing a known concentration of CH_2O with minimal contaminant species [32]. This characterization is detailed further in Section III.C. For studying the decomposition and oxidation of MMA, mixtures of MMA and O_2 in argon were prepared by evaporating liquid MMA from the interchangeable glass flask into the agitated mixing tank to a desired partial pressure (below MMA's vapor pressure of ~29 Torr) and subsequently filling the tank with either Ar or a mixture of Ar and O_2 .

An interband cascade laser (ICL, Nanoplus) with \sim 8.3 mW of output power is used to target absorbance features of CH₂O near 3.60 µm—shown in the left of Fig. 2, while an ICL (Nanoplus) with \sim 6 mW of output power targets CO₂ absorption features near 4.19 µm and a quantum cascade laser (QCL, ALPES Lasers) with \sim 50 mW of output power targets CO absorbance features near 4.98 µm. Laser light was pitched through the shock tube test section, spectral bandpass filters, irises, and focusing lenses onto photovoltaic (PV) detectors (VIGO System) as shown in the left of Fig. 3. The ICL targeting CH₂O provides a scan depth of 1.03 cm⁻¹ over a spectral range surrounding a collection of lines near 2778.5 cm⁻¹ comprising the $^{Q}Q_{5}$ branch of the v_{1} symmetric C–H stretch band and the $^{P}Q_{7}$ branch of

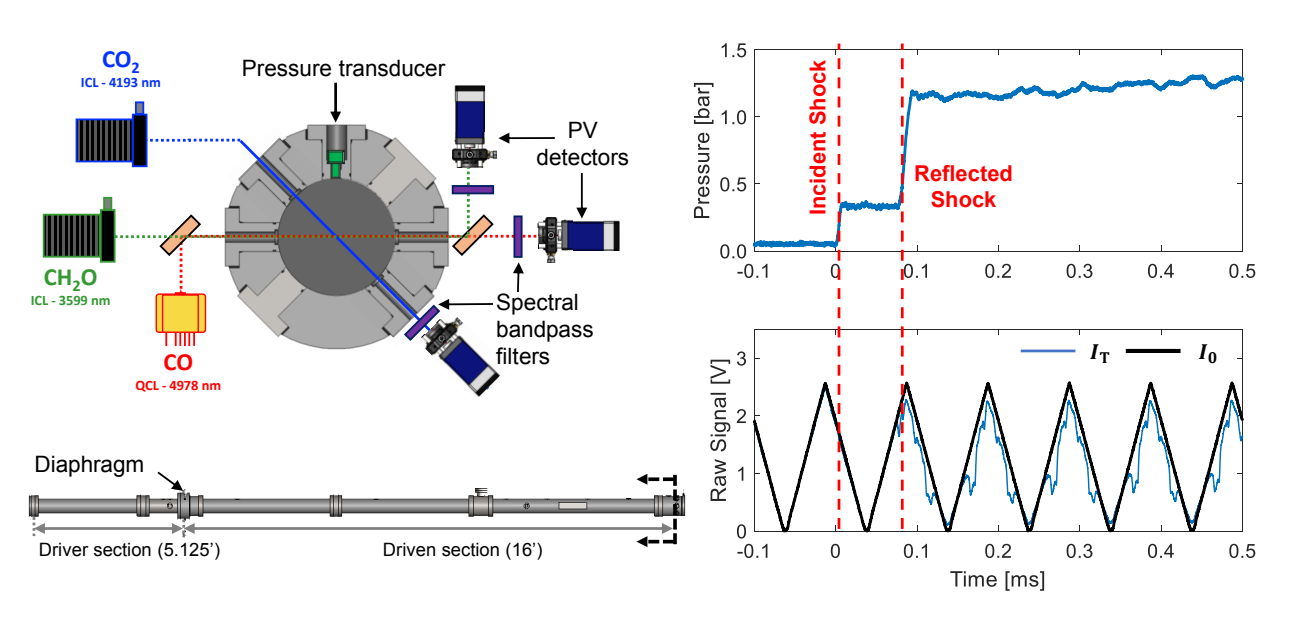


Fig. 3 Left: Cross-section of the shock tube test section (top) showing windows for optical access and laser/detector setup alongside side view of shock tube (bottom) showing location of the test section at the end of the driven section of the tube; Right: Representative time-histories of pressure (top) and PV detector intensity data (bottom) from a shock heated mixture of C₃H₆O₃.

the $v_2 + v_4$ combination band of CH₂O [33]. Likewise, the ICL targeting CO₂ provides a scan depth of 1.1 cm⁻¹ over the R(0,62) line of CO₂'s (01⁰0 \rightarrow 01⁰1) v_3 fundamental band near 2386 cm⁻¹, while the QCL provides a scan depth of 1.45 cm⁻¹ over the P(0,31) and P(2,20) lines of CO's fundamental band near 2008.5 cm⁻¹. These wavelength regions for CO₂ and CO have been targeted in previous investigations by the authors for temperature and concentration measurements in hybrid rocket flows [14, 15] and are not detailed further here. All lasers are scanned at 40 kHz using a triangle wave; both the up- and down-scan are leveraged to increase the effective measurement rate to 80 kHz; representative scans for both the incident (I_0) and transmitted (I_t) intensity of the 3.6 µm ICL are shown in the right of Fig. 3 alongside a corresponding dynamic pressure measurement.

C. Temperature-dependent cross-sections of formaldehyde near 3.6 µm

Experimental measurements of broadband CH₂O spectra at elevated temperatures (>300 K) in the literature are scarce, and accordingly there has been little experimental validation of available spectral databases for CH₂O in conditions relevant for hybrid rocket combustion, even for databases developed using computational chemistry explicitly for high temperatures [34, 35]. Moreover, collisional broadening parameters for the ro-vibrational transitions comprising the targeted spectral region—which are necessary for quantitative interpretation of the crowded spectra at even atmospheric pressures—are unavailable for an argon bath gas, which is typically employed in shock tube kinetic studies to achieve combustion-relevant temperatures behind reflected shock waves.

To characterize the high-temperature spectroscopy of CH₂O near 3.6 μm, mixtures of gaseous 1,3,5 Trioxane $(C_3H_6O_3)$ and argon were barometrically prepared by heating and sublimating solid $C_3H_6O_3$ to partial pressures less than or equal to 3.3 Torr (The vapor pressure of C₃H₆O₃ is 11 Torr) in the agitated mixing tank, followed by addition of inert Ar to create mixtures of 0.25–0.33% C₃H₆O₃ in Ar for shock-heating. These low partial pressures were chosen to avoid deposition of solid C₃H₆O₃ on the interior walls of the mixing tank, which was visually confirmed with imaging provided by an illuminated boroscope in the tank. C₃H₆O₃/Ar mixtures were then shock-heated to measure CH₂O absorption cross-sections $\sigma_{abs}(v, P, T)$ at 950–1510 K and 0.5 - 1.5 atm. Representative experimentally-obtained cross sections are shown in the middle of Fig. 4 alongside simulations utilizing the latest HITRAN and ExoMol spectral line lists. Simulations performed with the HITRAN line list were calculated assuming line-by-line broadening parameters available for air, while those performed with the ExoMol line list were calculated assuming broadening parameters for air averaged across all available data for the spectral region. The simulations using both state-of-the-art spectral models demonstrate significant disagreement with one another. We also suspect collisional line-mixing [36] is present in the $^{P}Q_{7}$ branch of the $v_{2} + v_{4}$ combination band of CH₂O, for which no spectral models are available in the literature and is difficult to characterize without experimental measurements. Fortuitously, this otherwise non-ideal line mixing behavior is observed to give rise to local regions of absorbance with very different temperature sensitivities across the targeted temperatures and pressures, as shown in the middle and right of Fig. 4.

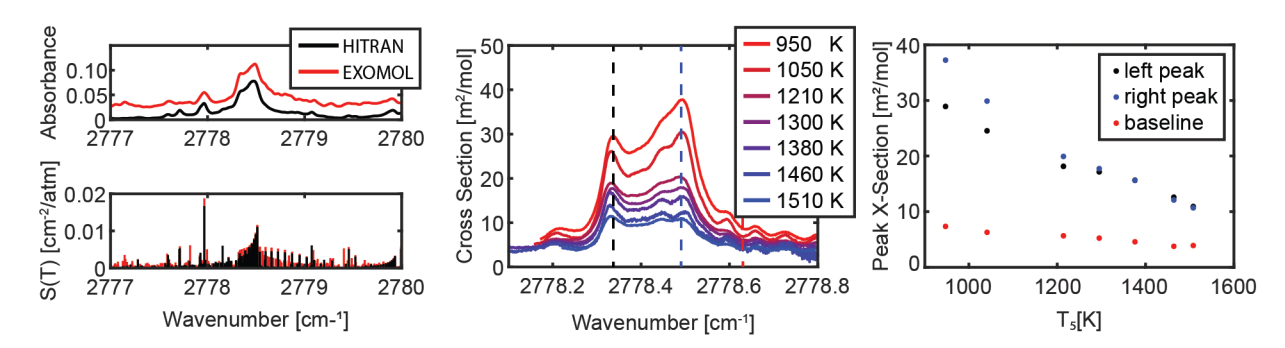


Fig. 4 Left: Predicted CH₂O absorbance (top) and linestrengths (bottom) at 1200 K and 1 atm in the spectral region of interest using parameters from the HITRAN2020 [26] and ExoMol [37] databases; Middle: CH₂O absorbance cross-sections for multiple temperatures, with wavelengths corresponding to local peaks annotated; Right: Temperature-dependence of cross-section peaks from 950–1500 K.

The temperature and pressure conditions for the cross-section measurements were selected to ensure that formaldehyde formed from the 1,3,5 Trioxane relatively quickly and remained constant during the test time, determined from the time evolution of the measured absorbance and informed by previous studies of formaldehyde absorbance with shock-heated 1,3,5 Trioxane [38, 39]. With the pressure and temperature determined as mentioned in Sec.III, the absorbance signals

can be normalized by number density $N_{\rm abs}$ and pathlength L to obtain $\sigma_{\rm abs}(\nu, P, T)$ for each measured test condition. Equipped with a database of spectrally-resolved temperature- and pressure-dependent absorbance cross-sections of CH₂O, the time histories of CH₂O mole fractions can be determined from CH₂O cross-sections experimentally measured during the decomposition and oxidation of MMA behind reflected shock waves.

IV. Results

Multiple shock tube experiments targeting the decomposition and oxidation of MMA were conducted for different temperatures, and some representative plots of species concentration evolution are shown in Fig. 5.

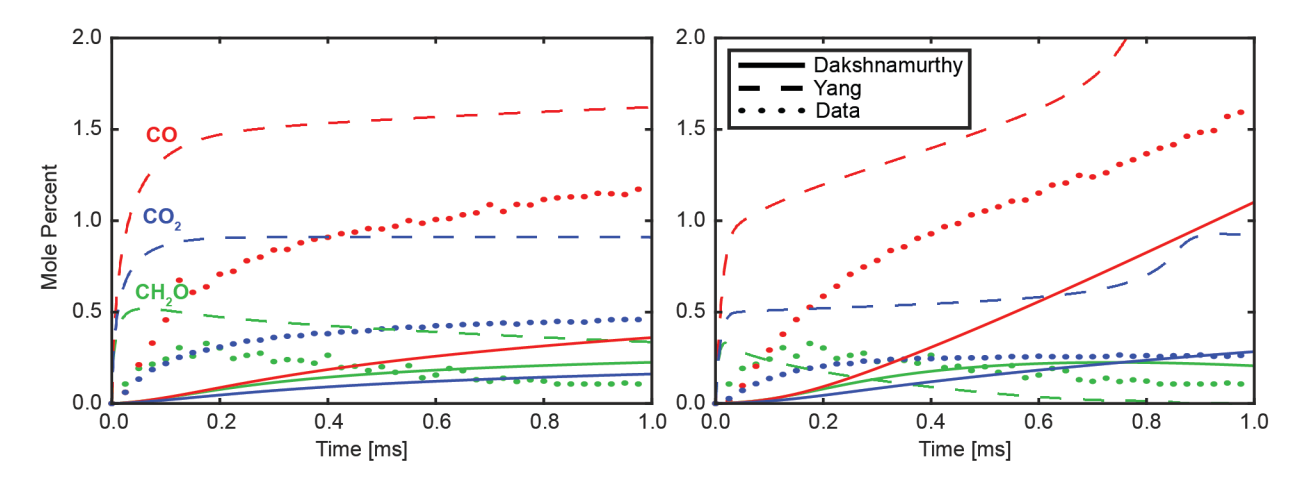


Fig. 5 Species time-histories of CH₂O (blue), CO (red), and CO₂ (blue) obtained by LAS (dotted line) during the decomposition or oxidation of MMA in argon compared to predictions by the kinetic models from Yang et al. [19] (solid lines) and Dakshnamurthy et al. [23] (dashed lines); *Left:* thermal decomposition of 2% MMA/Ar at 1400 K and 1 atm; *Right:* Oxidation of 1% MMA in 3% O₂/Ar at 1400 K and 1 atm.

The left of Fig. 5 depicts time histories of CO, CO₂, and CH₂O during the decomposition of 2% MMA in Ar over a 1 ms test time at an initial reflected shock temperature of 1400 K and pressure of 1 atm. CH₂O is observed to form rapidly, preceding the appearance of CO and CO₂, which also increase rapidly in concentration during the first fifth of the test. As the decomposition continues, the mole fraction of CH₂O peaks and decays slightly, while CO₂ increases slightly, and the mole fraction of CO increases markedly, exceeding the original number of moles of MMA in the mixture. The kinetic model by Yang et al. [19], shown as solid lines, is observed to over-predict all species concentrations and production rates during the initial decomposition of MMA, as well as over-predict the ratios of CO₂/CH₂O during the initial formation of CH₂O. Conversely, the reduced model by Dakshnamurthy et al. [23], shown as dashed lines, is observed to under-predict all species concentrations and production rates for the first half of the experiment, while it over-predicts just CH₂O concentration in the latter half of the experiment.

The right of Fig. 5 depicts the time histories of CO, CO₂, and CH₂O during the oxidation of 1% MMA in 3% O₂/Ar (corresponding to an equivalence ratio of $\phi = 2$) over a 1-ms test time at a similar initial reflected shock temperature of 1400 K and pressure of 1 atm. Fuel-rich conditions were chosen owing to their relevance in hybrid rocket combustion. As with the MMA decomposition, CH₂O initially forms more rapidly than CO and CO₂, but in this case it decays more rapidly over the course of the test time. The mole percent of CO₂ plateaus to around 0.25%, while the mole percent of CO increases throughout the test time. Similar to the decomposition experiment, the model by Yang et al. [19] over-predicts the production rate of all species at the start of the test time; however, qualitative behavior of all species is captured well up until about 0.8 ms, after which a second stage reaction event is predicted but not experimentally observed during the test time.

V. Summary and Future Work

In this work, laser absorption spectroscopy (LAS) techniques were developed and employed to study the reaction kinetics of methyl methacrylate (MMA, $C_5H_8O_2$) decomposition and oxidation though species time-history measurements

of formaldehyde (CH₂O, carbon monoxide (CO), and carbon dioxide (CO₂). A database of spectrally-resolved absorption cross-sections for CH₂O was first developed for temperature and concentration measurement in shock tube studies by shock-heating gaseous mixtures containing 1,3,5 trioxane (C₃H₆O₃) to produce a known concentration of CH₂O at multiple temperatures spanning 900–1600 K and pressures near 1 atm. The data were used to develop an empirical model for quantitative interpretation of CH₂O spectra obtained by LAS during the decomposition and oxidation of MMA at temperatures and mixture concentrations relevant to hybrid rocket combustion of solid poly(methyl methacrylate) (PMMA) fuel. In the experiments, established LAS techniques were used to additionally measure the time-histories of CO and CO₂ during MMA decomposition and oxidation. The LAS measurements of CH₂O, CO, and CH₂O were subsquently compared to state-of-the art chemical models for MMA combustion, revealing several shortcomings associated with model development that solely considers experimental validation against laminar flames. These data will provide critical kinetic constraints to current and future reaction mechanisms used to describe PMMA combustion in models of hybrid rocket propulsion systems.

Acknowledgements

This work was supported by the U.S. National Science Foundation, CAREER Award No. 1752516 and by the Air Force Office of Scientific Research (AFOSR) Young Investigator Program (YIP) award no. FA9550-19-1-0062 with Dr. Chiping Li as Program Officer. ICS acknowledges support from the The Natural Sciences and Engineering Research Council of Canada. Nicolas Q. Minesi acknowledges support from NASA's Space Technology Research Grants Program (award no. 80NSSC21K0066). The authors thank Prof. Sergey Yurchenko of University College London for helpful discussions regarding the latest ExoMol database for CH₂O.

References

- [1] Jens, E. T., Cantwell, B. J., and Hubbard, G. S., "Hybrid Rocket Propulsion Systems for Outer Planet Exploration Missions," *Acta Astronautica*, Vol. 128, 2016, pp. 119–130. doi:10.1016/j.actaastro.2016.06.036, URL http://dx.doi.org/10.1016/j.actaastro.2016.06.036.
- [2] Karp, A. C., Nakazono, B., Story, G., Chaffin, J., and Zilliac, G., "Hybrid Propulsion Technology Development for a Potential Near- Term Mars Ascent Vehicle," 2019 IEEE Aerospace Conference, Vol. 2019-March, IEEE, 2019, pp. 1–8. doi:10.1109/AERO.2019.8741854.
- [3] Jens, E. T., Karp, A. C., Miller, V. A., Hubbard, G. S., and Cantwell, B. J., "Experimental Visualization of Hybrid Combustion: Results at Elevated Pressures," *Journal of Propulsion and Power*, Vol. 36, No. 1, 2020, pp. 33–46. doi:10.2514/1.B37416.
- [4] Lazzarin, M., Faenza, M., Barato, F., Bellomo, N., Bettella, A., and Pavarin, D., "Computational Fluid Dynamics Simulation of Hybrid Rockets of Different Scales," *Journal of Propulsion and Power*, Vol. 31, No. 5, 2015, pp. 1458–1469. doi: 10.2514/1.B35528.
- [5] Mahottamananda, S. N., Kadiresh, N. P., and Pal, Y., "Regression Rate Characterization of HTPB-Paraffin Based Solid Fuels for Hybrid Rocket," *Propellants, Explosives, Pyrotechnics*, 2020, p. prep.202000051. doi:10.1002/prep.202000051.
- [6] Karabeyoglu, A., "Challenges in the Development of Large-scale Hybrid Rockets," *International Journal of Energetic Materials and Chemical Propulsion*, Vol. 16, No. 3, 2017, pp. 243–261. doi:10.1615/IntJEnergeticMaterialsChemProp.2018022732.
- [7] Mazzetti, A., Merotto, L., and Pinarello, G., "Paraffin-based Hybrid Rocket Engines Applications: A Review and a Market Perspective," *Acta Astronautica*, Vol. 126, 2016, pp. 286–297. doi:10.1016/j.actaastro.2016.04.036.
- [8] Seshadri, K., and Williams, F. A., "Structure and extinction of counterflow diffusion flames above condensed fuels: Comparison between poly(methyl methacrylate) and its liquid monomer, both burning in nitrogen-air mixtures," *Journal of Polymer Science: Polymer Chemistry Edition*, Vol. 16, No. 7, 1978, pp. 1755–1778. doi:10.1002/pol.1978.170160726, URL http://doi.wiley.com/10.1002/pol.1978.170160726.
- [9] Fernandez-Pello, A. C., and Hirano, T., "Controlling mechanisms of flame spread," *Combustion Science and Technology*, Vol. 32, No. 1-4, 1983, pp. 1–31. doi:10.1080/00102208308923650.
- [10] Kim, S., Lee, J., Moon, H., Kim, J., Sung, H., and Kwon, O. C., "Regression Characteristics of the Cylindrical Multiport Grain in Hybrid Rockets," *Journal of Propulsion and Power*, Vol. 29, No. 3, 2013, pp. 573–581. doi:10.2514/1.B34619.

- [11] Bhargava, A., Van Hees, P., and Andersson, B., "Pyrolysis modeling of PVC and PMMA using a distributed reactivity model," *Polymer Degradation and Stability*, Vol. 129, 2016, pp. 199–211. doi:10.1016/j.polymdegradstab.2016.04.016, URL http://dx.doi.org/10.1016/j.polymdegradstab.2016.04.016.
- [12] Fraters, A., and Cervone, A., "Experimental Characterization of Combustion Instabilities in High-Mass-Flux Hybrid Rocket Engines," *Journal of Propulsion and Power*, Vol. 32, No. 4, 2016, pp. 958–966. doi:10.2514/1.B35485.
- [13] Mechentel, F. S., Hord, B. R., and Cantwell, B. J., "Optically Resolved Fuel Regression of a Clear Polymethylmethacrylate Hybrid Rocket Motor," *Journal of Propulsion and Power*, Vol. Article in, 2020, pp. 1–10. doi:10.2514/1.B37805.
- [14] Bendana, F. A., Sanders, I. C., Castillo, J. J., Hagström, C. G., Pineda, D. I., and Spearrin, R. M., "In-situ thermochemical analysis of hybrid rocket fuel oxidation via laser absorption tomography of CO, CO2, and H2O," *Experiments in Fluids*, Vol. 61, No. 9, 2020, p. 190. doi:10.1007/s00348-020-03004-7.
- [15] Sanders, I. C., Bendana, F. A., Hagström, C. G., and Mitchell Spearrin, R., "Injector Effects on Hybrid Polymethylmethacrylate Combustion Assessed by Thermochemical Tomography," *Journal of Propulsion and Power*, Vol. 37, No. 6, 2021, pp. 928–943. doi:10.2514/1.B38316, URL https://arc.aiaa.org/doi/10.2514/1.B38316.
- [16] Bendana, F. A., Sanders, I. C., Stacy, N. G., and Spearrin, R. M., "Localized characteristic velocity (c*) for rocket combustion analysis based on gas temperature and composition via laser absorption spectroscopy," *Measurement Science and Technology*, Vol. 23, No. 6, 2021, pp. 149–152. doi:10.1088/1361-6501/ac18d3, URL https://iopscience.iop.org/article/10.1088/1361-6501/ac18d3.
- [17] Wang, T., Li, S., Lin, Z., Han, D., and Han, X., "Experimental study of laminar lean premixed methylmethacrylate/oxygen/argon flame at low pressure," *Journal of Physical Chemistry A*, Vol. 112, No. 6, 2008, pp. 1219–1227. doi:10.1021/jp709927j.
- [18] Lin, Z., Wang, T., Han, D., Han, X., Li, S., Li, Y., and Tian, Z., "Study of combustion intermediates in fuel-rich methyl methacrylate flame with tunable synchrotron vacuum ultraviolet photoionization mass spectrometry," *Rapid Communications in Mass Spectrometry*, Vol. 23, No. 1, 2009, pp. 85–92. doi:10.1002/rcm.3838, URL https://onlinelibrary.wiley.com/doi/10.1002/rcm.3838.
- [19] Yang, B., Westbrook, C., Cool, T., Hansen, N., and Kohse-Höinghaus, K., "Photoionization mass spectrometry and modeling study of premixed flames of three unsaturated C5H8O2 esters," *Proceedings of the Combustion Institute*, Vol. 34, No. 1, 2013, pp. 443–451. doi:10.1016/j.proci.2012.05.034, URL https://linkinghub.elsevier.com/retrieve/pii/ S1540748912000351.
- [20] Knyazkov, D. A., Bolshova, T. A., Shvartsberg, V. M., Chernov, A. A., and Korobeinichev, O. P., "Inhibition of premixed flames of methyl methacrylate by trimethylphosphate," *Proceedings of the Combustion Institute*, Vol. 38, No. 3, 2021, pp. 4625–4633. doi:10.1016/j.proci.2020.06.048, URL https://doi.org/10.1016/j.proci.2020.06.048.
- [21] Law, C. K., Combustion Physics, Cambridge University Press, New York, 2006.
- [22] Won, S. H., Windom, B., Jiang, B., and Ju, Y., "The role of low temperature fuel chemistry on turbulent flame propagation," *Combustion and Flame*, Vol. 161, No. 2, 2014, pp. 475–483. doi:10.1016/j.combustflame.2013.08.027, URL http://dx.doi.org/10.1016/j.combustflame.2013.08.027.
- [23] Dakshnamurthy, S., Knyazkov, D. A., Dmitriev, A. M., Korobeinichev, O. P., Nilsson, E. J., Konnov, A. A., and Narayanaswamy, K., "Experimental Study and a Short Kinetic Model for High-Temperature Oxidation of Methyl Methacrylate," *Combustion Science and Technology*, Vol. 191, No. 10, 2019, pp. 1789–1814. doi:10.1080/00102202.2018.1535492.
- [24] Hill, P. G., and Peterson, C. R., *Mechanics and Thermodynamics of Propulsion*, 2nd ed., Addison-Wesley Publishing Co, Reading, MA, 1992.
- [25] Hanson, R., and Davidson, D., "Recent advances in laser absorption and shock tube methods for studies of combustion chemistry," *Progress in Energy and Combustion Science*, Vol. 44, 2014, pp. 103–114. doi:10.1016/j.pecs.2014.05.001.
- [26] Gordon, I., Rothman, L., Hargreaves, R., Hashemi, R., Karlovets, E., Skinner, F., Conway, E., Hill, C., Kochanov, R., Tan, Y., Wcisło, P., Finenko, A., Nelson, K., Bernath, P., Birk, M., Boudon, V., Campargue, A., Chance, K., Coustenis, A., Drouin, B., Flaud, J., Gamache, R., Hodges, J., Jacquemart, D., Mlawer, E., Nikitin, A., Perevalov, V., Rotger, M., Tennyson, J., Toon, G., Tran, H., Tyuterev, V., Adkins, E., Baker, A., Barbe, A., Canè, E., Császár, A., Dudaryonok, A., Egorov, O., Fleisher, A., Fleurbaey, H., Foltynowicz, A., Furtenbacher, T., Harrison, J., Hartmann, J., Horneman, V., Huang, X., Karman, T., Karns, J., Kassi, S., Kleiner, I., Kofman, V., Kwabia–Tchana, F., Lavrentieva, N., Lee, T., Long, D., Lukashevskaya, A., Lyulin, O., Makhnev, V., Matt, W., Massie, S., Melosso, M., Mikhailenko, S., Mondelain, D., Müller, H., Naumenko,

- O., Perrin, A., Polyansky, O., Raddaoui, E., Raston, P., Reed, Z., Rey, M., Richard, C., Tóbiás, R., Sadiek, I., Schwenke, D., Starikova, E., Sung, K., Tamassia, F., Tashkun, S., Vander Auwera, J., Vasilenko, I., Vigasin, A., Villanueva, G., Vispoel, B., Wagner, G., Yachmenev, A., and Yurchenko, S., "The HITRAN2020 molecular spectroscopic database," *Journal of Quantitative Spectroscopy and Radiative Transfer*, Vol. 277, 2022, p. 107949. doi:10.1016/j.jqsrt.2021.107949, URL https://linkinghub.elsevier.com/retrieve/pii/S0022407321004416.
- [27] Rothman, L., Gordon, I., Barber, R., Dothe, H., Gamache, R., Goldman, A., Perevalov, V., Tashkun, S., and Tennyson, J., "HITEMP, the High-Temperature Molecular Spectroscopic Database," *Journal of Quantitative Spectroscopy and Radiative Transfer*, Vol. 111, No. 15, 2010, pp. 2139–2150. doi:10.1016/j.jqsrt.2010.05.001.
- [28] Bendana, F. A., Lee, D. D., Wei, C., Pineda, D. I., and Spearrin, R. M., "Line mixing and broadening in the v(1→3) first overtone bandhead of carbon monoxide at high temperatures and high pressures," *Journal of Quantitative Spectroscopy and Radiative Transfer*, Vol. 239, 2019, p. 106636. doi:10.1016/j.jqsrt.2019.106636.
- [29] Pineda, D. I., Bendana, F. A., Schwarm, K. K., and Spearrin, R. M., "Multi-isotopologue laser absorption spectroscopy of carbon monoxide for high-temperature chemical kinetic studies of fuel mixtures," *Combustion and Flame*, Vol. 207, 2019, pp. 379–390. doi:10.1016/j.combustflame.2019.05.030.
- [30] Campbell, M. F., Owen, K. G., Davidson, D. F., and Hanson, R. K., "Dependence of Calculated Postshock Thermodynamic Variables on Vibrational Equilibrium and Input Uncertainty," *Journal of Thermophysics and Heat Transfer*, Vol. 31, No. 3, 2017, pp. 586–608. doi:10.2514/1.T4952.
- [31] Irdam, E. A., and Kiefer, J. H., "The decomposition of 1,3,5-trioxane at very high temperatures," Chemical Physics Letters, Vol. 166, No. 5-6, 1990, pp. 491–494. doi:10.1016/0009-2614(90)87139-I.
- [32] Alquaity, A. B., Giri, B. R., Lo, J. M., and Farooq, A., "High-Temperature Experimental and Theoretical Study of the Unimolecular Dissociation of 1,3,5-Trioxane," *Journal of Physical Chemistry A*, Vol. 119, No. 25, 2015, pp. 6594–6601. doi:10.1021/acs.jpca.5b01801.
- [33] Pine, A. S., "Doppler-limited spectra of the CH stretching fundamentals of formaldehyde," *Journal of Molecular Spectroscopy*, Vol. 70, No. 2, 1978, pp. 167–178. doi:10.1016/0022-2852(78)90151-0.
- [34] Al-Refaie, A. F., Yachmenev, A., Tennyson, J., and Yurchenko, S. N., "ExoMol line lists VIII. A variationally computed line list for hot formaldehyde," *Monthly Notices of the Royal Astronomical Society*, Vol. 448, No. 2, 2015, pp. 1704–1714. doi:10.1093/mnras/stv091, URL http://academic.oup.com/mnras/article/448/2/1704/1059875/ExoMol-line-lists-VIII-A-variationally-computed.
- [35] Al-Derzi, A. R., Tennyson, J., Yurchenko, S. N., Melosso, M., Jiang, N., Puzzarini, C., Dore, L., Furtenbacher, T., Tóbiás, R., and Császár, A. G., "An improved rovibrational linelist of formaldehyde, H212C16O," *Journal of Quantitative Spectroscopy and Radiative Transfer*, Vol. 266, 2021, p. 107563. doi:10.1016/j.jqsrt.2021.107563, URL https://doi.org/10.1016/j.jqsrt.2021.107563https://linkinghub.elsevier.com/retrieve/pii/S002240732100056X.
- [36] Hartmann, J. M., Boulet, C., and Robert, D., Collisional Effects on Molecular Spectra, Elsevier, 2008. doi:10.1016/B978-0-444-52017-3.X0001-5. URL https://linkinghub.elsevier.com/retrieve/pii/B9780444520173X00015.
- [37] Tennyson, J., Yurchenko, S. N., Al-Refaie, A. F., Barton, E. J., Chubb, K. L., Coles, P. A., Diamantopoulou, S., Gorman, M. N., Hill, C., Lam, A. Z., Lodi, L., McKemmish, L. K., Na, Y., Owens, A., Polyansky, O. L., Sousa-Silva, C., Underwood, D. S., Yachmenev, A., and Zak, E., "The ExoMol database: molecular line lists for exoplanet and other hot atmospheres," *Journal of Molecular Spectroscopy*, Vol. 327, 2016, pp. 73–94. doi:10.1016/j.jms.2016.05.002, URL http://dx.doi.org/10.1016/j.jms.2016.05.002http://arxiv.org/abs/1603.05890.
- [38] Wang, S., Davidson, D. F., and Hanson, R. K., "High-temperature laser absorption diagnostics for CH2O and CH3CHO and their application to shock tube kinetic studies," *Combustion and Flame*, Vol. 160, No. 10, 2013, pp. 1930–1938. doi:10.1016/j.combustflame.2013.05.004, URL http://dx.doi.org/10.1016/j.combustflame.2013.05.004.
- [39] Ding, Y., Wang, S., and Hanson, R. K., "Sensitive and interference-immune formaldehyde diagnostic for high-temperature reacting gases using two-color laser absorption near 5.6 μm," *Combustion and Flame*, Vol. 213, 2020, pp. 194–201. doi:10.1016/j.combustflame.2019.11.042, URL https://doi.org/10.1016/j.combustflame.2019.11.042.